

EXPERIMENTAL AND THEORETICAL SPECTROSCOPIC STUDIES, CHARGE DISTRIBUTION ANALYSIS OF SINGLE LAYERED GRAPHENE

M. SARANYA^a, S. AYYAPPAN^{a*}, R.NITHYA^a, A.GOKILA^b,
R. K. SANGEETHA^b

^a*Department of Physics, Government college of Technology, Coimbatore, 641013,
India*

^b*Department of Physics, Sri Eshwar College of Engineering, Coimbatore, 608002,
India*

Vibrational wavenumber assignments and geometrical parameters of single layer graphene (SLG) were investigated using density functional theory (DFT) with the basis set of 6-31G (d,p). The scaled vibrational assignments are found to be in good agreement with experimental values. The excitation energy, oscillator strength and wavelength were calculated using time dependent density functional theory (TD-DFT) and compared with the experimental UV-Vis spectra. The total density of states (TDOS) and partial density of states (PDOS) of the molecules were studied. The highest occupied molecular orbital (HOMO), lowest unoccupied molecular orbital (LUMO) and molecular electrostatic potential mapping also analysed.

(Received November 25, 2016; Accepted February 6, 2017)

Keywords: SLG, TDOS, PDOS, HOMO-LUMO, MESP

1. Introduction

Graphene is the fundamental building block for every type of carbon, for example, graphite, fullerene and carbon nanotubes. After the revelation of graphene by Andre Geim and Konstantin Novoselov in 2004, it produced a great interest for graphene and its applications [1]. A solitary graphene sheet is a planar monolayer of sp²-fortified carbon molecules organized on a two-dimensional honeycomb grid made of hexagonal rings [2]. The discovery of graphene begins from its special physicochemical properties, eminently the incredibly high surface area, warm versatility and mechanical quality [3]. Regardless, the promising electronic properties of graphene have activated innovative work for its utilization in novel optical devices [4], electronic devices [5], photocatalytic materials [6], ecological sensors [7], vitality creation and storage [8]. Graphene is the favoured medium by physicists and materials researchers, because of its simple arrangement and process capacity [9]. For tentatively portraying the oxygen-containing bunches, computational techniques are of awesome offer assistance. Quantum computational techniques have turned into a promising device for the investigation of sub-atomic structure holding, compliances, steadiness and response instrument. Quantum mechanical expectation of atomic properties has its wide use in concoction issues, inferable from the advancement in PC equipment and productive computational programming. Gaussian is the most broadly utilized program bundle, for performing electronic structure figuring's. In the present work, sub-atomic geometry, nuclear charges and vibrational spectra, re-enacted utilizing Gaussian'98 (Version 09) programming, has been utilized for the definite sub-atomic auxiliary and vibrational ghastry investigation. Numerous exploratory and hypothetical gatherings have indicated bunches of intrigue and clarified the way of holding and reactivity of the framework. The majority of the clarifications depended on some natural thoughts and exact tenets that were basically gotten from a few exploratory perceptions and numerous compound responses. Henceforth, the need for a natural and right hypothetical approach for these ideas was inescapable. In this study, introduce the view of Hartree Fock and B3LYP calculated for

* Corresponding author: ayyappan@gct.ac.in

Single Layered Graphene (SLG) and a factual approach of some auxiliary properties to examine in particular geometrical parameters, structure and vibrational assignments.

2. Computational details

The quantum chemical calculation method is used to predict the vibrational wavenumbers and HOMO-LUMO studies using B3LYP method with the basis set 6-31G (d,p) [10] Gaussian 09 software programs [11]. The vibrational wavenumber assignments were carried out by the result analysed by Gaussview Program [12]. The calculated FTIR and Raman spectra were obtained using pure Lorentzian-band and its bandwidth range of 10cm^{-1} . The UV-Visible spectrum of the SLG is calculated using time dependent density functional theory.

3. Experimental details

X-ray diffraction (XRD) were recorded at room temperature at the filtering rate of $0.02^\circ/\text{min}$ for the range from 10° – 80° utilizing PANalytical X'Pert-Pro diffractometer with Cu $K\alpha_1$ radiation ($\lambda=1.5406 \text{ \AA}$). The infrared spectra of the examples were acquired by utilizing a Fourier change infrared (FTIR) spectrometer (Bruker Tensor 27, Germany) with a working range of 400 cm^{-1} – 4000 cm^{-1} in a KBr pellet technique. The Raman spectra were analysed using JY-1058 Raman spectrometer with excitation wavelength of 520 nm as a laser source with a extent up to 4000 cm^{-1} . The UV-visible spectra were carried out using JoscoV-650 spectrophotometer in the wavelength regime of 400 – 800 nm .

4. Results and discussion

4.1 Geometrical parameters

A powder X-ray diffraction spectrum of single layered graphene was shown in figure 1. The diffraction peak of this molecule was found at $2\theta=26.3^\circ$ which corresponded graphite structure. The optimized molecular structure parameters such as bond length and bond angles of the single layer graphene were calculated by B3LYP at basis set 6-31G(d,p) method are shown in figure 1. From the literature survey, the bond length of graphene is reported as 1.43 \AA [13]. The SLG consists of carbon sp^2 hybridisation of single and double bonding atoms. Generally, single C-C bonding in aromatic ring structure will not have the same bond lengths and bond angles [14]. The bond length of the C-C and C=C approximately lies in the range of 1.5079 \AA and 1.3443 \AA respectively. The bond angles of the single and double bond carbon atoms were nearly 120° and 117° respectively [15-16].

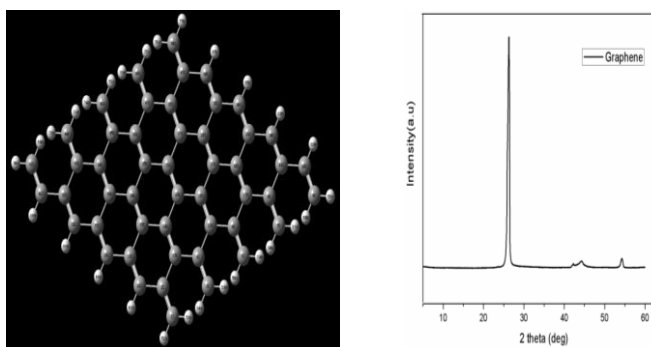


Fig. 1 Geometrical molecular structure and experimental XRD pattern of SLG

4.2 UV-Vis analysis and HOMO LUMO studies

The time dependent density functional theory (TD-DFT) methods were used to determine the low lying excited state of the title of the compound is fully optimized ground state structure [17]. The calculation involving excitation energy wavelength and oscillator strength have been carried out and compare with experimental data are shown in Table 1. The experimental and computed UV-Vis spectrum and the atomic composition of the frontier molecular orbital between various energy gap levels were shown in figure 2.

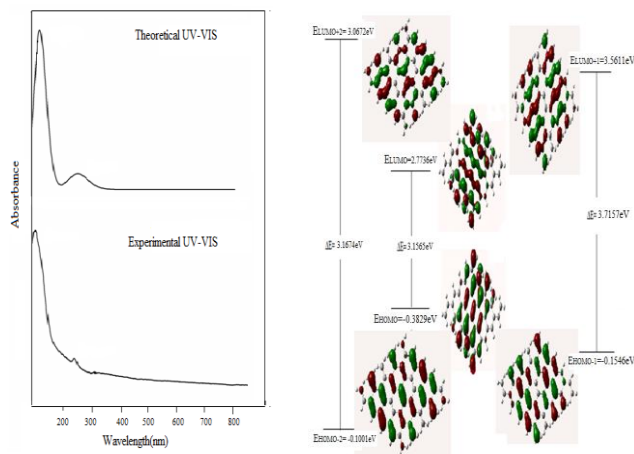


Fig. 2. Theoretical and experimental UV-Vis absorbance spectra of SLG and frontier molecular orbital diagram of SLG.

The UV absorption spectra of the single layered graphene were calculated by time dependent density functional theory at the basis set of (d, p). The results compliment with the experimental finding. The UV analyse is the major contribution among the energies of HOMO and LUMO. The experimental absorption peaks were obtained at 195, 303 and 350 nm corresponding to the computed UV absorption spectra of the title of the molecule are 191 and 239 nm by TD-DFT B3LYP method which is also good agreement to each other. The electronic absorption spectra corresponds to the transition from molecular orbital were the highest occupied molecular orbital and the lowest unoccupied molecular orbital of title of the compound are alpha molecular orbital level (164) and alpha molecular orbital level (165) respectively. The HOMO energy determine the ability of donor of an electron and LUMO determine the ability of accept of an electron respectively [18]. The HOMO LUMO energy gap is lower implies the kinetic energy is lower, so that the molecule is stable because it is energetically electrons add a low lying LUMO and receiving the electron from higher lying HOMO. The HOMO and LUMO were computed by B3LYP/6-31G (d,p) levels. The HOMO-LUMO has been used to prove the bioactivities from intramolecular charge transfer within the molecules. The energy values of HOMO (164) orbital and LUMO (165) orbital were lying at an energy value of -0.3829 eV and 2.7736 eV respectively. The electron charge transition takes place from HOMO orbital (164) to LUMO orbital (165) and this energy transition implies charge transfer from C=C to C-C of the title of the molecule. The HOMO-LUMO energy gap was obtained at 3.1565 eV in the isolated gas molecular calculations. The calculated self consistent field (SCF) energy gap of the title of the compound is -1886.226 a.u. With this energy gap, it can be said that the title of the compound has low kinetic stability and high chemical reactivity.

Table 1 Experimental and computed absorption wavelength (λ), excitation energies (E) and oscillator strength (f) of SLG by B3LYP/6-31G (d, p) method

Exp wavelength (nm)	Theoretical wavelength (nm)	Excitation level	Transition state	Transition energy (nm)	Excitation energy	Oscillator strength
350	-	I	161→ 165	23.2257	3.6109	0
			163→ 165	5.6966		
			164→ 166	8.53145		
			164→ 168	33.0079		
303	239	II	162→ 165	9.5078	3.638	0.2353
			163→ 164	10.9665		
			164→ 165	6.3362		
			164→ 167	13.6219		
195	191	III	162→ 163	35.3807	4.2744	2.3834
			162→ 165	12.4527		
			163→ 166	8.8565		
			164→ 165	6.6065		
			164→ 167	-13.6699		

Table 2 Theoretical transition levels between HOMO and LUMO and frontier orbital of single layered graphene calculated by B3LYP/6-31G (d,p) method

Level	MO Energy (eV)	Level	MO Energy (eV)	ΔE (eV)
HOMO	-0.3829	LUMO	2.7736	3.1565
HOMO	-0.3829	LUMO+1	3.5611	3.9440
HOMO	-0.3829	LUMO+2	3.0672	3.4501
HOMO-1	-0.1546	LUMO	2.7736	2.9282
HOMO-2	-0.1001	LUMO	2.7736	2.8738
HOMO-1	-0.1546	LUMO+1	3.5611	3.7157
HOMO-2	-0.1001	LUMO+2	3.0672	3.1674

4.3 Vibrational analysis

4.3.1 CH vibrations

The experimental and computed FT-IR and FT-RAMAN spectrum were shown in figure 3. The geometrical aromatic of the title of the compound shows the presence of CH stretching vibration in the range of 3100 to 3000cm^{-1} which is the characterization identification of CH stretching vibration. From the SLG molecule, there are four CH bonds [19] such as CH stretching, CH in-plane and CH out plane bending vibrations corresponding to C11-H62, C21-H64, C31-H66, C20-H63, C30-H65, C40-H64 respectively. Hence, in our present work, the experimental FT-IR spectrum observes 3028 , 2929 , 2864cm^{-1} is assigned to CH stretching vibrations. The scaled wavenumber calculated by B3LYP6-31(d, p). Method predicts at 3036 , 3021 , 2998 , 2997cm^{-1} show good agreement with the experimental values. The CH in plane bending [20] acquired in the region of 1430 - 990cm^{-1} and it is very useful to the study of characterization purposes. The CH in plane bending vibration associates with CC stretching vibrations and the range is 1000 - 1300cm^{-1} . In this work, the peak is assigned at FTIR are 1061cm^{-1} . However, the wavenumber assigned for CH in plane bending shows good agreement with the theoretical wavenumber values at 1397 , 1394 , 1261 , 1245 and 1138cm^{-1} by B3LYP 6-31(d,p) basis set. The CH out plane bending [21] and the ring absorption band of the SLG is calculated between 960 - 771cm^{-1} . By comparing

experimental and theoretical frequencies by B3LYP method denotes that the peaks are shifted above from the expected range due to the vibrations of more aromatic rings in this molecule.

4.3.2 C-C vibrations and C=C vibrations

The expected range of carbon CC stretching vibrations [22] in the range of 1300 -1400 cm^{-1} . This CC vibration is coupled with in plane bending vibrations of the ring. Hence, it is assigned at 1440-1377 cm^{-1} . The FT-Raman absorbed at 1354 cm^{-1} coincides to the theoretical values. The double bond C=C carbon stretching vibrations [23] band present in between 1432-1650 cm^{-1} . The carbon CC stretching vibrations present in FTIR spectra and FT-Raman spectra 1620 and 1590 cm^{-1} respectively. The C=C double bond stretching vibrations of the present compound were calculated by B3LYP method are the IR spectra band 1654 and 1690 cm^{-1} and raman band spectra range from 1674 and 1548 cm^{-1} . The theoretical and experimental value of the C-C stretching vibration of the graphene shows good viability result.

4.3.3 Raman intensities

The prediction of raman activities of SLG are computed by B3LYP method using Gaussian program. From the theory of raman scattering [24-25], the raman activities were converted into relative raman intensity using the relationship as

$$I_i = \frac{f(\nu_o - \nu_i)^4 S_i}{\nu_i(1 - \exp^{h\nu_i/KT})}$$

Where ν_o is the exciting wavenumber in cm^{-1} , ν_i is the vibrational wavenumber of the i th normal mode, h , c and k are fundamental constants, S_i is the raman activity and f is a suitably chosen common normalization factor for all peak intensities. The calculated relative intensities of FT-IR and FT-Raman were shown in the figure 3 and table 3.

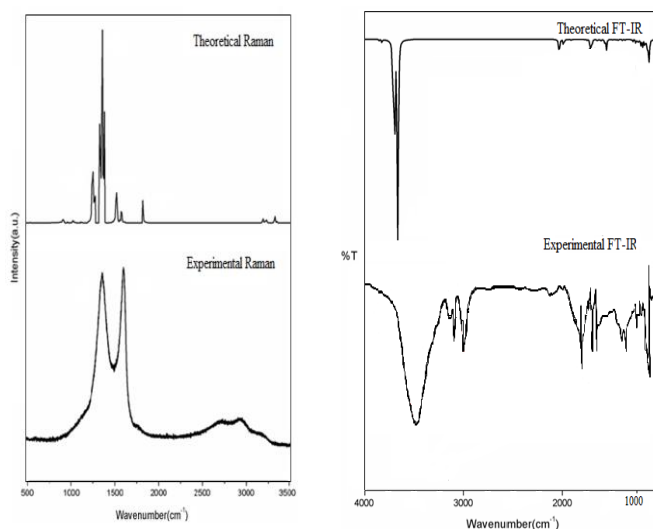


Fig. 3 Theoretical and experimental FT-IR and FT-RAMAN spectra of SLG

Table 3 Experimental and computed wave number, IR and Raman intensity and vibrational assignments obtained for single layered graphene at B3LYP/6-31G (d, p) method

Wave number (cm ⁻¹)				Intensity (abs)				Vibrational assignment
Theoretical value		Experimental value		Experimental value		Theoretical value		
IR	RAMAN	IR	RAMAN	IR	RAMAN	IR	RAMAN	
3036						183.94		v C-H
3021						446.48		v C-H
2998						247.35		v C-H
2997						358.59		v C-H
	1674						142.98	v C-C
1654						58.49		v C-C
	1632						3539.88	v C-C
	1622						5740.80	v C-C
1619		1620		0.55		14.66		v C-C
	1617						3829.14	v C=C
	1604						6136.51	β-C=C
	1581		1590		310.00		16122.87	β-C=C
	1548						2186.27	v C=C
	1440						1103.96	β H-C-H
1397						18.16		β CH
1394						17.12		β C-H
	1386						909.73	β C-H
	1377		1354		314.0		1174.18	v C-C
1261						30.15		β C-C
1245		1061		0.65		22.58		β C-H
	1138						482.92	β C-H
960						34.21		β C-C-C
	918						287.72	β C-C
906						57.97		β C-H
771						8.96		β C-H

v- stretching; β- bending ; τ- torsion

4.4. Density of states (DOS)

The important application of DOS plot is to demonstrate the molecular orbital and their contribution of chemical bonding through the PDOS plot [26]. The DOS plot results show that overlapping population in the molecular orbital. The OPDOS result shows that non bonding,

bonding and antibonding interactions between the two orbital atom groups. The positive value of OPDOS indicating that the bonding interaction and negative value indicates the antibonding interactions and zero values indicates the non bonding interactions. The DOS plot gives the composition of group of orbital contributing to the molecular orbital. The PDOS and OPDOS plots are shown in the figure 4. The plot for DOS is taken from the range of -1.50a.u. to $+1.50\text{a.u.}$ The graph exhibits the orbital characteristics of different energy range. It is the major contribution from s orbital and p orbital basic function of carbon in the frontier molecular orbital. The partial density of states (PDOS) of the carbon atom of the title of the molecule exhibits the total density states of the molecules. The PDOS of the carbon has just larger positive energy then the negative energy values. The OPDOS curve is in the negative region shows antibonding characteristic of the molecule. This is due to unfavourable in orbital as seen from LUMO isosurface. The DOS of the title of the molecules overlapped to partial DOS of the carbon atoms.

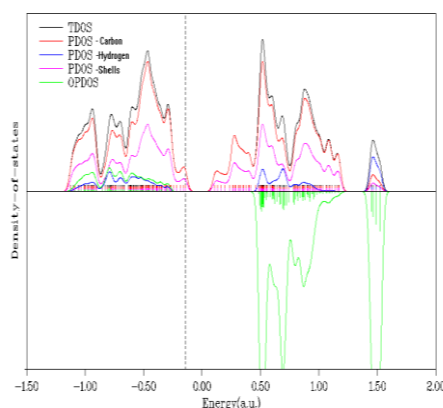


Fig. 4 Total and partial density of states diagram of SLG

4.5 Molecular electrostatic potential

The molecular electrostatic potential (MESP) of the title of the molecule is calculated by B3LYP with the basis set (d, p). The MESP of the title of the molecule is the method for analysing and predicting molecular reactive behaviours of various biological systems and its hydrogen bonding interaction. The MESP has been applied extensively to the investigation of the reactive behaviour of both nucleic acids and bases and for increasing larger fragments of DNA and RNA nucleic acids. Electrostatic potential maps illustrate the charge distributions of molecules three dimensionally. These maps allow us to visualize variable charged regions of a molecule. The negative electrostatic potential corresponds to attraction of proton by concentrated electron density of the molecules. It depends on lone pairs and π bond interactions. The positive electrostatic potential corresponds to repulsion of proton by atomic nucleus in the region. It depends on low electron density and incomplete nuclear charge of the molecules. The MESP at different points on the electron density isosurface is shown by the colour isosurface in the figure 5. The red colour code surface provides the information about the region of negative value potential and blue surface region provides electrophilic attraction in the region of positive potential likely to be attracted by nucleophilic attractions.

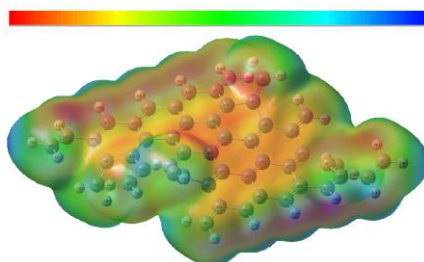


Fig. 5 Molecular electrostatic potential mapping of SLG

5. Conclusions

In this study, experimental and calculated normal mode vibrations have been analysed. The calculated FT-IR, FT-Raman and UV-Vis spectra of the SLG have been analyzed. Observed and calculated wave numbers are found to be in good agreement. The experimental and theoretical UV-Vis spectrum provides insight into the excitation energy and oscillator strength were calculated and it shows the carbon-carbon bonding and electron transitions helps to the charge transfer in intramolecular of the SLG.

The density of states of the title of the compound were analysed and it exhibits the stabilization of the molecule which depends on carbon atoms. The MESP mapping provides the information on charge density distribution and the chemical reactivity of the molecule.

References

- [1] K.S. Novoselov, A.K. Geim, S. V. Morozov, et.al., *Science* **306**, 666 (2004).
- [2] G. J. Guan, S. Y. Zhang, S. H. Liu, et.al., *Chem. Soc.* **137**, 6152 (2015).
- [3] Y. B. Sun, Q. Wang, C. L. Chen, X. L. Tan, *Environ. Sci. Technol.* **46**, 6020 (2012).
- [4] X. Li, W. Cai, J. An, S. Kim, R.S. Ruoff, *Science* **324**, 1312 (2009).
- [5] Z. Wu, W. Ren, L. Gao, B. Liu, C. Jiang, H. Cheng, *Carbon* **47**, 493 (2009).
- [6] H.C. Schniepp, J.L. Li, M.J. McAllister, H. Sai, *J. Phys. Chem. B* **110**, 8535 (2006).
- [7] K.S. Kim, Y. Zhao, H. Jang, S.Y. Lee, et.al., *Nature* **457**, 706 (2009).
- [8] NA. Kotov, *Materials science, Nature* **442**, 254 (2006).
- [9] A. Gopalakrishnan, R. Krishnan, S. Thangavel, *J. Ind. Eng. Chem.* **30**, 14 (2015).
- [10] B. Miehllich, A. Savin, H. Stroll, H. Preuss, *Chem. Phys. Lett.* **157**, 200 (1989).
- [11] M.Frisch, et al , *Gaussian an 09 ,Rev.,E.,01*, 2009
- [12] A. Frish, A.B. Nielson, A.J. Holder, *GASSVIEW view*, Gaussian Inc., 2000.
- [13] Weidong Wang, Yuxiang Zhang, Cuili Shen, *AIP Advances* **6**, 025317 (2016).
- [14] Lin-Vien, Daimay, et al. Elsevier, 1991.
- [15] Wang, Junmei, et al., *Journal of molecular graphics and modelling* **25.2**, 247 (2006).
- [16] Saito, R., et al., *Applied physics letters* **60.18**, 2204 (1992).
- [17] Stratmann, R. Eric, et.al., *The Journal of Chemical Physics* **109.19**, 8218 (1998).
- [18] Casida, Mark E., Kim C. Casida, et.al., *Int. journal of quantum chemistry* **70.405**, 933 (1998).
- [19] Lui, Chun Hung, et al. *Nano letters* **12.11**, 5539 (2012).
- [20] Scherer, James R., and John Overend. *Spectrochimica Acta* **17.7**, 719 (1961).
- [21] Suzuki, Isao. *Bulletin of the Chemical Society of Japan* **35.9**, 1449 (1962).
- [22] Paraschuk, D. Yu, V. M. Kobryanskii. *Physical review letters* **87.20**, 207402 (2001).
- [23] Wilson, E. Bright, John Courtney Decius, Courier Corporation, 2012.
- [24] G. Keresztury, S. Holly, J. Varga, et.al., *Spectrochim. Acta* **9A**, 2007 (1993).
- [25] G. Keresztury, J.M. Chalmers, vol. 1, John Wiley & Sons Ltd., New York, 2002.
- [26] J. W. Mintmire, C. T. White, *Physical Review Letters* **81.12**, 2506 (1998).